



## Research paper

# N-acetyl cysteine reverts the proinflammatory state induced by cigarette smoke extract in lung Calu-3 cells

Ángel G. Valdivieso<sup>a,\*</sup>, Andrea V. Dugour<sup>b</sup>, Verónica Sotomayor<sup>a</sup>, Mariángeles Clauzure<sup>a</sup>, Juan M. Figueroa<sup>b</sup>, Tomás A. Santa-Coloma<sup>a,\*</sup>

<sup>a</sup> Institute for Biomedical Research (BIOMED, UCA-CONICET), Laboratory of Cellular and Molecular Biology, School of Medical Sciences, Pontifical Catholic University of Argentina (UCA) and The National Scientific and Technical Research Council of Argentina (CONICET), Alicia Moreau de Justo 1600, Buenos Aires C1107AFF, Argentina

<sup>b</sup> Fundación Pablo Cassará, Buenos Aires, Argentina



## ARTICLE INFO

## Keywords:

Cigarette smoke extract

Mitochondria

CFTR

ROS

COPD

Cystic fibrosis

## ABSTRACT

Chronic obstructive pulmonary disease (COPD) and cystic fibrosis (CF) are lethal pulmonary diseases. Cigarette consumption is the main cause for development of COPD, while CF is produced by mutations in the *CFTR* gene. Although these diseases have a different etiology, both share a CFTR activity impairment and proinflammatory state even under sterile conditions. The aim of this work was to study the extent of the protective effect of the antioxidant N-acetylcysteine (NAC) over the proinflammatory state (IL-6 and IL-8), oxidative stress (reactive oxygen species, ROS), and CFTR levels, caused by Cigarette Smoke Extract (CSE) in Calu-3 airway epithelial cells. CSE treatment (100 µg/ml during 24 h) decreased *CFTR* mRNA expression and activity, and increased the release of IL-6 and IL-8. The effect on these cytokines was inhibited by N-acetyl cysteine (NAC, 5 mM) or the NF-κB inhibitor, IKK-2 (10 µM). CSE treatment also increased cellular and mitochondrial ROS levels. The cellular ROS levels were normalized to control values by NAC treatment, although significant effects on mitochondrial ROS levels were observed only at short times (5') and effects on CFTR levels were not observed. In addition, CSE reduced the mitochondrial NADH-cytochrome c oxidoreductase (mCx I-III) activity, an effect that was not reverted by NAC. The reduced CFTR expression and the mitochondrial damage induced by CSE could not be normalized by NAC treatment, evidencing the need for a more specific reagent. In conclusion, CSE causes a sterile proinflammatory state and mitochondrial damage in Calu-3 cells that was partially recovered by NAC treatment.

## 1. Introduction

Smoking, both active and passive, is the mayor non-infectious cause of respiratory disease and constitutes a risk factor for respiratory infections. Chronic obstructive pulmonary disease (COPD) is caused by environmental and genetic factors, and is characterized by chronic cough, respiratory secretions and progressive dyspnea and fibrosis, produced by chronic exposure of susceptible individuals to cigarette smoke (CS) [1]. The risk of disease increases proportionally to the amount of cigarettes smoked per day, although other factors, such as high exposure to dust, chemicals, and genetic factors (mutations in the

$\alpha_1$ -antitrypsin gene), could promote COPD [2].

Even though they are of different etiology, COPD shares similar respiratory symptoms with Cystic Fibrosis (CF) [1]. CF is an autosomal recessive disease [3] caused by mutations in the cystic fibrosis transmembrane conductance regulator (*CFTR*) gene, which encodes a chloride channel regulated by adenosine triphosphate (ATP) and 3',5'-cyclic adenosine monophosphate (cAMP) [4,5]. Both, COPD and CF, are characterized by airflow limitation, strong inflammatory response, recurrent infections, and progressive loss of lung function [1]. In the last years, several reports show that COPD is also associated with alterations in the CFTR channel function [1,6–12]. Studies in CF suggest that

**Abbreviations:** ATP, adenosine triphosphate; cAMP, 3',5'-cyclic adenosine monophosphate; CF, cystic fibrosis; cROS, cytoplasmic ROS; CFTR, cystic fibrosis transmembrane conductance regulator; mCx-I-III, mitochondrial NADH-cytochrome c oxidoreductase; COPD, Chronic obstructive pulmonary disease; CS, cigarette smoke; CSE, cigarette smoke extract; CTCF, corrected total cell fluorescence; DCFH-DA, 2',7'-dichlorofluorescein diacetate; DMSO, dimethyl sulfoxide; EDTA, ethylenediaminetetraacetic acid; FBS, fetal bovine serum; HEPES, 4-(2-hydroxyethyl)-1-piperazineethanesulfonic acid; IBMX, 3-isobutyl-1-methylxanthine; mCx-I, mitochondrial Complex I; MOPS, 3-(N-morpholino)propanesulfonic acid; mtROS, mitochondrial ROS; MTS, [3-(4,5-dimethylthiazol-2-yl)-5-(3-carboxymethoxyphenyl)-2-(4-sulfophenyl)-2H-tetrazolium, inner salt]; NAC, N-acetyl cysteine; OXPHOS, oxidative phosphorylation system; PBS, phosphate buffered saline; PMSF, phenylmethylsulfonyl fluoride; ROS, reactive oxygen species; RQ, relative quantification; RT-qPCR, quantitative real-time RT-PCR; SPQ, 6-methoxy-N-[3-sulfopropyl]quinolinium

\* Corresponding authors.

E-mail addresses: [angel\\_valdivieso@uca.edu.ar](mailto:angel_valdivieso@uca.edu.ar) (Á.G. Valdivieso), [tomas\\_santacoloma@uca.edu.ar](mailto:tomas_santacoloma@uca.edu.ar), [tsantacoloma@gmail.com](mailto:tsantacoloma@gmail.com) (T.A. Santa-Coloma).

<https://doi.org/10.1016/j.redox.2018.03.006>

Received 12 December 2017; Received in revised form 9 March 2018; Accepted 13 March 2018

Available online 14 March 2018

2213-2317/ © 2018 The Authors. Published by Elsevier B.V. This is an open access article under the CC BY license (<http://creativecommons.org/licenses/by/4.0/>).

the impairment of the CFTR is associated with an alteration of the mitochondrial function, in particular the mitochondrial complex I (mCx-I) activity and reactive oxygen species (ROS) production [13–18]. The extent to which CF and COPD share similar pathological mechanisms could be of interest to identify new therapeutic targets for both diseases.

A common adverse characteristic of COPD and CF is a strong inflammatory response, initiated with the increased secretion of proinflammatory cytokines and ROS levels [1]. In the treatment of respiratory diseases, the antioxidant N-acetylcysteine (NAC) has emerged as a mucolytic, antioxidant and anti-inflammatory drug [19,20]. NAC antioxidant effects occurs directly, through its free sulfhydryl group that serves as a source of reducing equivalents, and indirectly, through the replenishment of intracellular GSH levels [21]. In fact, NAC acts as a cysteine precursor for the synthesis of glutathione (GSH), increasing the antioxidant protection of the cells [22].

The aim of this work was to study the extent of the protective effect of the antioxidant N-acetylcysteine (NAC) over the proinflammatory state and oxidative stress caused by CSE [7,19,23]. For this purpose we used cultured Calu-3 airway cells as a model system, measuring the secretion of the cytokines IL-6 and IL-8 as proinflammatory markers [23]. Calu-3 cells express high levels of CFTR [24] and constitute a good *in vitro* model to study human respiratory function, inflammatory responses and diseases [25]. In cells exposed to CSE, we observed an increased IL-6 and IL-8 secretion induced through NF- $\kappa$ B activation, together with a reduced CFTR expression and activity. The reduction in the CFTR expression could not be reverted by NAC. However, the increased secretion of these cytokines was blocked by NAC, suggesting that ROS contributed to the NF- $\kappa$ B activation. We also demonstrated a fast induction of the mitochondrial ROS levels (mtROS) and a later mitochondrial NADH cytochrome c oxidoreductase (Complex I-III) activity impairment that could not be improved with NAC treatment. The NAC effects over ROS and cytokine levels suggest that an antioxidant treatment may help to reduce inflammation in COPD; it also evidences the need for an antioxidant therapy directed to specifically reduce the mitochondrial oxidative stress and damage to the oxidative phosphorylation system (OXPHOS) induced by CSE, which was not reverted with NAC treatment. On the other hand, the possible CFTR role in the proinflammatory response is not clear yet.

## 2. Materials and methods

### 2.1. Chemicals

Dimethyl sulfoxide (DMSO, culture grade), valinomycin, dibutyryl-cAMP, IBMX (3-isobutyl-1-methylxanthine), cytochrome c and (-)-isoproterenol hydrochloride were purchased from Sigma-Aldrich (St. Louis, MO). Trypsin was purchased from Life Technologies (GIBCO BRL, Rockville, MD) and SPQ (6-methoxy-N-[3-sulfopropyl]quinolinium) from Invitrogen (Carlsbad, CA). MitoSOX and 2',7'-dichlorofluorescein diacetate (DCFH-DA) was from Molecular Probes (Eugene, OR). The IKK-2 inhibitor SC-514 (CAS 354812–17-2) was from Calbiochem (San Diego, CA). Cigarette smoke extract (CSE) (stock solution 40 mg/ml in DMSO) was from Murty Pharmaceuticals (Lexington, KY). N-acetylcysteine (NAC) (0.5 M stock solution in water (pH = 7.4)) was purchased from PharmaZell (PharmaZell, Chennai und Vizag, India). All other reagents were analytical grade. The stock solutions of valinomycin, IBMX, and dibutyryl-cAMP were prepared at 1000 $\times$  in culture-grade DMSO. Isoproterenol was dissolved in water at 1000 $\times$  concentration.

### 2.2. Cell culture

Calu-3 cells (ATCC Cat# HTB55), epithelial airway cells known to express wt-CFTR [24], were used in the experiments. Cells were cultured in DMEM (Life Technologies, GIBCO BRL, Rockville, MD)

supplemented with 10% FBS (Life Technologies, GIBCO BRL, Rockville, MD), 100 U/ml penicillin, 100  $\mu$ g/ml streptomycin, and 0.25  $\mu$ g/ml amphotericin B (GIBCO BRL).

### 2.3. CSE exposure

Cells were incubated with CSE at the concentrations and times indicated for each assay. For viability assays, 10–200  $\mu$ g/ml CSE were used for various times (5–72 h). For the rest of the experiments, cells were exposed to 100  $\mu$ g/ml CSE during 24 h since this concentration and time did not negatively affect viability. Control cells contained the same final amount of DMSO (0.25%) [26] as in CSE exposed cells.

### 2.4. Cell viability and proliferation assays

Calu-3 cells were grown in 96-well plates (10,000 cells/cm<sup>2</sup> in 100  $\mu$ l of DMEM-10% FBS medium). The cells were incubated with different concentrations of CSE (10, 50, 100 and 200  $\mu$ g/ml), or the vehicle (DMSO) at different times (0, 5, 24, 48 and 72 h). We used a commercial cigarette smoke extract (CSE) to assure the reproducibility of the assays. Cell viability was evaluated by using the CellTiter 96<sup>®</sup> Aqueous One Solution Cell Proliferation Assay (Promega, Madison, WI), according to manufacturer's instructions. Briefly, after washing with PBS, pH 7.4, cells were treated with staining solution containing the tetrazolium compound MTS [3-(4,5-dimethylthiazol-2-yl)–5-(3-carboxymethoxyphenyl)–2-(4-sulfophenyl)–2H-tetrazolium, inner salt] and an electron coupling reagent (phenazine ethosulfate; PES). Absorbance was recorded at 490 nm using a microplate reader (model Benchmark, Bio-Rad, Hercules, CA).

### 2.5. Quantitative real-time RT-PCR (RT-qPCR)

To determine CFTR mRNA expression levels, RT-qPCRs were performed and the  $\Delta\Delta$ Ct method was used for comparative quantification, as previously described [17,27]. Briefly, total RNA (4  $\mu$ g) from Calu-3 cells, treated with 100  $\mu$ g/ml CSE or vehicle for 24 h, was used for reverse transcription by using M-MLV Reverse Transcriptase (Promega) and Oligo-dT, according to the manufacturer's instructions (100 U of RT/ $\mu$ g of RNA). PCR conditions were performed as previously described [17,27]. qRT-PCR reactions were carried out in an Applied Biosystems 7500 Real-Time PCR equipment, and thermocycler conditions were: denaturation at 94  $^{\circ}$ C (5 min), and 40 cycles of 94  $^{\circ}$ C (30 s), 60  $^{\circ}$ C (30 s), and 72  $^{\circ}$ C (30 s).

### 2.6. CFTR transport activity in Calu-3 cells

The fluorescent probe SPQ was used to measure the CFTR chloride transport activity, as we previously described [17,27,28], with some modifications. Calu-3 cells were seeded at a density of 40,000 cells/cm<sup>2</sup> in 2 ml of medium and grown at confluence in p6 wells plates containing one rectangular coverslips (22  $\times$  8 mm, from Hitachi) pre-treated with a coating solution (10  $\mu$ g/ml fibronectin, 4.4  $\mu$ g/ml collagen, 1.5  $\mu$ g/ml BSA in DMEM/F12). The cells were incubated with 100  $\mu$ g/ml CSE or the vehicle for 24 h. Cells were loaded with SPQ by hypotonic shock by using 5 mM SPQ (dissolved 1:1 in serum-free DMEM/F12:H<sub>2</sub>O distilled and sterile, washed three times with NaI buffer (135 mM NaI, 10 mM Glucose, 1 mM CaSO<sub>4</sub>, 1 mM MgSO<sub>4</sub>, 10 mM HEPES, 2.4 mM K<sub>2</sub>HPO<sub>4</sub>, and 0.6 mM KH<sub>2</sub>PO<sub>4</sub>, pH 7.4)) and maintained in NaI at 37  $^{\circ}$ C for 30 min. The measurement of the CFTR activity was performed as previously described [28]. Data was plotted as F/Fi – 1 vs time (F: fluorescence; Fi: initial fluorescence measured after the NaI buffer perfusion). The halide efflux slopes were estimated by using the initial 6 points of time after the CFTR response to stimulation started.

## 2.7. Secretion of IL-8 and IL-6

Calu-3 cells were seeded (27,000 cells/cm<sup>2</sup> in 100 µl of DMEM-10% FBS medium) in 96 well-plates and grown to confluence. The cells were then incubated with 100 µg/ml CSE, 100 µg/ml CSE plus 10 µM IKK-2 inhibitor, 100 µg/ml CSE plus 5 mM NAC or the vehicle for 24 h. IL-6 and IL-8 were measured from supernatants using the human IL-6 and IL-8 ELISA set (BD OptEIA™ - Human IL-8 ELISA Set, and BD OptEIA™ - Human IL-6 ELISA Set, BD Biosciences, San Diego, CA). Measurements were performed using a microplate reader according to manufacturer's instructions (model Benchmark, Bio-Rad).

## 2.8. Cellular reactive oxygen species (ROS)

Cellular ROS levels were measured using the fluorescent probe DCFH-DA in cells cultured in 96-well plates (Greiner Bio-One, Germany; 655,090) as previously reported [13]. Briefly, 27,000 cells/cm<sup>2</sup> were seeded and grown to confluence in DMEM – 10% FBS medium. Then, cells were incubated in Hank's buffer containing 10 µM of DCFH-DA and incubated at 37 °C in a 5% CO<sub>2</sub>/air incubator for 40 min. Then, cells were washed five times with Hank's buffer and treated for 1 h with DMSO as vehicle, 100 µg/ml CSE or 100 µg/ml CSE plus 5 mM NAC. The fluorescence was measured at different times to determine the maximal signal in a fluorescence plate reader (NOVostar BMG LABTECH GmbH, Ortenberg, Germany) at 37 °C. Filters were Ex = 510 ± 10 nm, Em = 540 ± 10 nm and readings were performed by using 10 cycles (3 flashes per well and cycle; excitation and measurements were done from the bottom of the plate).

## 2.9. Confocal microscopy for cytoplasmic ROS measurement

To test the intracellular fluorescence signal and discard background, the DCF fluorescence was observed in a Zeiss LSM 510 confocal microscope (Plan-Neofluar 100×/1.3 Oil objective) (Carl Zeiss, Jena, Germany). Briefly, Calu-3 cells were seeded (27,000 cells/cm<sup>2</sup>) on chambered coverglasses (4-chamber, Nunc, Cat. No. 155383, Lab-Tek, Thermo Fisher Scientific, Rochester, NY) and cultured in DMEM-10% FBS medium. Cells were incubated in Hank's buffer containing 10 µM of DCFH-DA and incubated at 37 °C in a 5% CO<sub>2</sub>/air incubator for 40 min. Then, cells were washed with 0.4 ml of Hank's buffer five times and incubated with vehicle, 100 µg/ml CSE or 100 µg/ml CSE plus 5 mM NAC for 1 h. Cell images were acquired by using a LSM 510 Zeiss confocal microscope with a laser line of 488 nm and a long-pass filter LP505. The detector gain, offset, laser potency and pinhole were maintained for all conditions to compare the fluorescence intensity.

## 2.10. Confocal microscopy for mitochondrial ROS measurement

To measure mtROS, cells were cultured as above indicated for DCFH-DA, changing the probe to MitoSOX (5 µM), and incubating at 37 °C in a 5% CO<sub>2</sub>/air incubator for 10 min. Then, cells were washed with Hank's buffer four times (one minute each) and incubated in 100 µl of Hank's buffer. *In vivo* time-lapse images were acquired before the treatments with a final concentration of 100 µg/ml CSE or 100 µg/ml CSE plus 5 mM NAC. Confocal images were acquired in the LSM 510 confocal microscope by using a Plan-Neofluar 100×/1.3 Oil objective, a 488 nm laser line, and a long-pass (LP) filter of 560 nm (filter LP560). The detector gain, offset, laser potency and pinhole size were maintained for all conditions to compare the fluorescence intensity. ImageJ (<http://imagej.nih.gov/>) was used to quantify total fluorescence intensity by using corrected total cell fluorescence (CTCF) [26,29,30].

## 2.11. Mitochondria isolation

Mitochondria were isolated by using differential centrifugations as was previously described [13,17,31]. Briefly, cells were seeded at a

density of 25,000 cells/cm<sup>2</sup> (p100 dishes have 60 cm<sup>2</sup>) and cultured for 24 h in 5 ml DMEM- 10% FBS, at 37 °C in a humidified air atmosphere containing 5% CO<sub>2</sub>. Then, cells were washed with PBS, scrapped and centrifuged at 600 ×g for 5 min at 4 °C. The pellet was resuspended in isolation buffer (0.25 M sucrose, 25 mM MOPS, pH 7.4) and the cells were permeabilized by adding 0.12% w/v digitonin for 30 s on ice. The samples were diluted in three volumes of isolation buffer and centrifuged at 10,000 ×g for 20 min at 4 °C. The resultant pellet was re-suspended in 500 µl of isolation buffer and centrifuged at 800 ×g for 10 min at 4 °C. The supernatant was centrifuged at 10,000 ×g for 20 min at 4 °C, and the mitochondrial pellet was resuspended in 10–20 µl of BN-sample buffer A (1 M aminocaproic acid, 50 mM bis-Tris-HCl, 10 µM pepstatin, 10 µM leupeptin, 100 µM PMSF, 1 mM EDTA, pH 7.0) [13,17]. Mitochondrial protein concentration was measured by Lowry [32] by using aliquots of mitochondrial extract incubated with 0.1 N NaOH for 30 min at 37 °C, to dissolve mitochondrial membranes.

## 2.12. Spectrophotometric determination of mitochondrial NADH-cytochrome c reductase (mCx-I-III) activity

The NADH-cytochrome c reductase activity (mCx-I plus mCx-III) was spectrophotometrically measured in mitochondria from Calu-3 cells treated with 100 µg/ml CSE, 100 µg/ml CSE plus 5 mM NAC or vehicle for 24 h, in the presence/absence of rotenone (10 µM), as it was previously described [13,33,34]. Briefly, mitochondrial preparations were subjected to three freeze-thaw cycles to make them permeable to substrates. To measure the mCx-I-III activity, the mitochondria (equivalent to 100 µg of proteins) were resuspended in buffer solution (100 mM H<sub>2</sub>KPO<sub>4</sub>/HK<sub>2</sub>PO<sub>4</sub>, 0.5 mM KCN, 200 µM NADH, 25 µM oxidized cytochrome c, at pH 7.4). The reduction of cytochrome c was recorded by monitoring the increase in absorbance per minute for 2 min at 550 nm and 30 °C, and expressed as percentage, considering the activity in control cells as 100%. To determine the mCx-I activity, inhibition of NADH cytochrome c reductase activity by rotenone (10 µM) was measured in each sample after 5 min of preincubation with the inhibitor and the remaining values (insensitive to rotenone) were subtracted from the total activity.

## 2.13. Statistics

Unless otherwise indicated, all the assays were performed in duplicates and the experiments were repeated at least three times (n = 3). RT-qPCR reactions were carried out by using intra-assay triplicates. The final RT-qPCR quantification values were obtained as the means of the relative quantification (RQ) values for each independent experiment (n = 3). One-way ANOVA and Tukey's *post-hoc* test was applied to determine significant differences among samples (p < 0.05). All values are shown as mean ± SEM; the n value (number of replicates) is indicated in each case.

## 3. Results

### 3.1. Effects of CSE on Calu-3 cells viability

First, we measured the effects of continuous exposure to several concentrations of CSE on Calu-3 cells viability. As shown in Fig. 1A, plotting survival (%) vs CSE concentration (µg/ml), cell viability was significantly diminished only after 72 h of exposure to 100 or 200 µg/ml (p < 0.001). Similarly, plotting survival (%) vs time (Fig. 1B), a significant inhibition was observed with 100 and 200 µg/ml CSE (~27% and ~35% respectively) after 72 h of exposure (p < 0.001). In view of these results, we decided to run further experiments with the sublethal concentration of 100 µg/ml CSE during 24 h. Treatments for 24 h with NAC (5 mM), or CSE (100 µg/ml) + NAC (5 mM), did not have effects on cell viability (Supplementary Fig. 1).

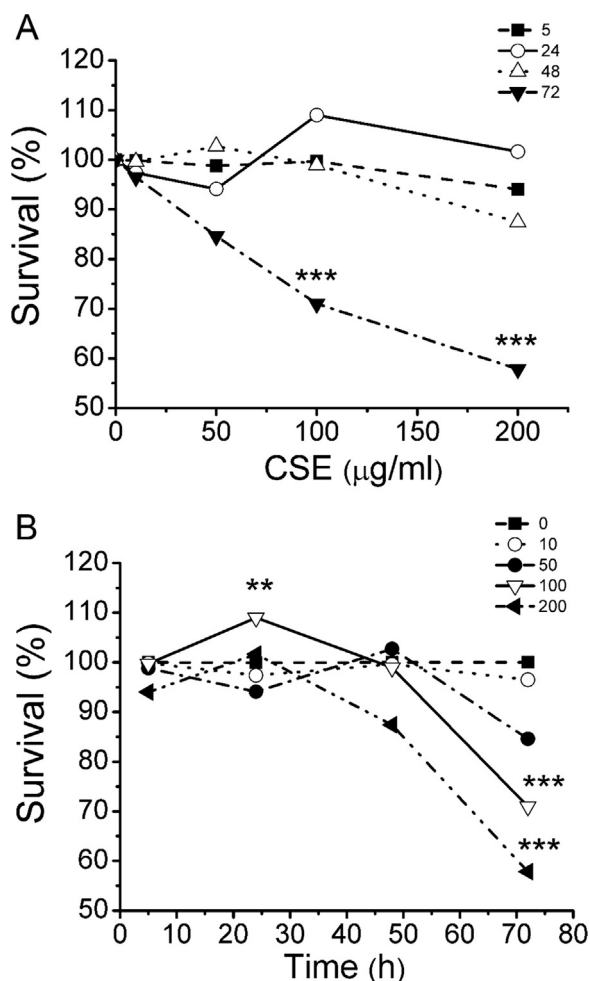


**Fig. 1.** Cell viability in Calu-3 cells exposed to CSE. **A:** Dose-response cell viability for CSE exposure (0, 10, 50, 100, and 200 µg/ml) at different times (5 dash line, 24 solid line, 48 dot line and 72 dash dot line h). **B:** Survival vs time plot for CSE exposure at different CSE concentrations (0 dash line, 10 dot line, 50 dash dot line, 100 solid line, and 200 dash dot line µg/ml). Viability was expressed as survival percentage (%) referred to control cells without CSE treatment (vehicle) as 100%. \*\* indicates  $p < 0.01$  and \*\*\*  $p < 0.001$  compared to control (untreated) cells ( $n = 4$ ). Statistical analyses were performed by ANOVA and Tukey's test.

### 3.2. CSE affects CFTR expression and activity

Low CFTR levels have been recently associated with COPD [1,10]; therefore, we wanted to validate the use of Calu-3 cells as a model for COPD measuring CFTR mRNA expression and activity after CSE exposure. As shown in Fig. 2A, the CFTR mRNA in cells exposed to 100 µg/ml of CSE for 24 h was reduced ( $p < 0.001$ ,  $n = 4$ ) compared to control cells (vehicle). On the other hand, NAC had not effects on the CFTR mRNA levels decreased by CSE treatment (Fig. 2A).

Then, to test if the decreased CFTR mRNA expression caused by CSE was reflected in an impairment of the CFTR function, the activity of the channel was measured by using the chloride sensitive fluorescent probe SPQ. As shown in Fig. 2B, the CSE treatment decreased both the basal and the cAMP-stimulated chloride efflux. The halide efflux slopes, that reflects the activation state of the channel, also showed a lower CFTR activation in Calu-3 cells treated with CSE (slope =  $0.012 \pm 0.001$ ;  $n = 3$ ) compared to control cells (DMSO treated cells) (slope =  $0.030 \pm 0.001$ ;  $n = 3$ ). In Fig. 2C, the halide efflux slopes were expressed as percentage referred to control cells as 100%. Thus, cells treated with CSE showed a significant ( $p < 0.05$ ) decrease, near to 60%, in the activity of the CFTR compared to control cells.

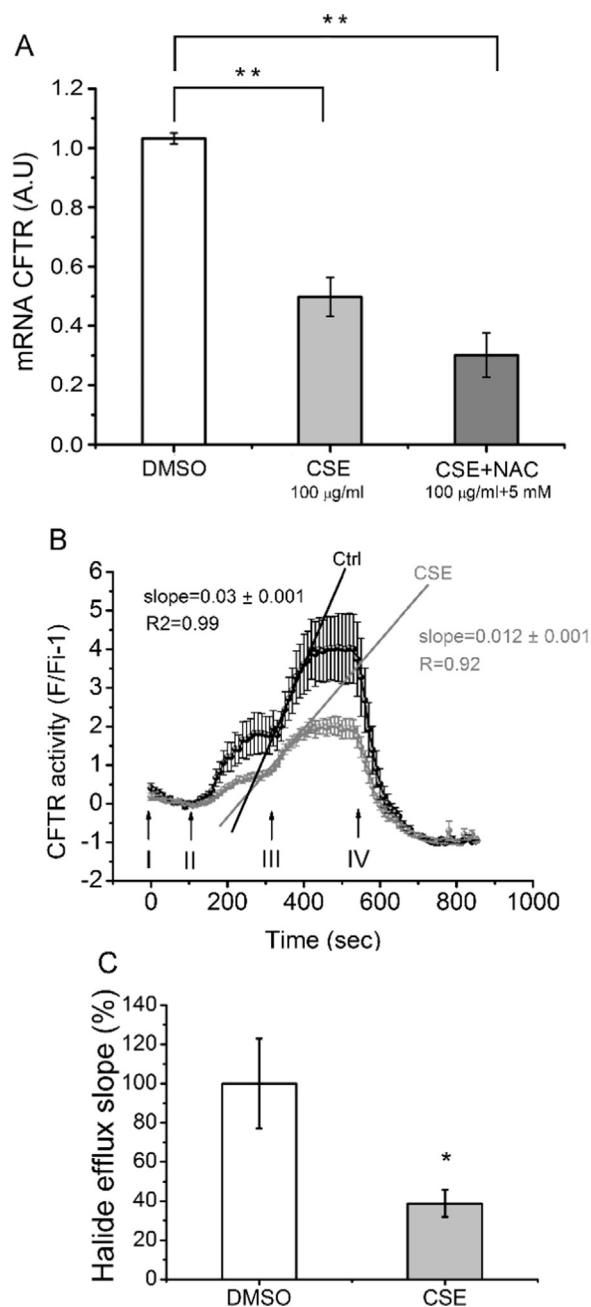


**Fig. 2.** CSE inhibit CFTR mRNA expression and activity. **A:** CFTR mRNA levels in Calu-3 cells treated with 100 µg/ml CSE (Cigarette Smoke Extract) or DMSO (vehicle) for 24 h, measured by quantitative real-time RT-PCR (qRT-PCR). The results were expressed as arbitrary units (A.U.). Measurements correspond to four independent experiments ( $n = 4$ ), each done in duplicate. **B:** CFTR channel halide transport activity was measured in Calu-3 cells treated with 100 µg/ml CSE or DMSO by using the SPQ Cl<sup>-</sup> sensitive probe. Arrows indicate the times of buffers addition; I: NaI buffer, II: NaNO<sub>3</sub> buffer, III: NaNO<sub>3</sub> buffer + cAMP cocktail, IV: KSCN 150 mM + 5 µM valinomyacin. Fluorescence values were calculated as  $F = (F-F_q)/(F_i-F_q) - 1$ ;  $F_i$  are the initial fluorescence values in NaI buffer.  $F_q$  corresponds to background values (fluorescence quenching in the presence of KSCN + valinomyacin). The graph is the mean of four independent experiments ( $n = 4$ ). **C:** Halide efflux slopes, corresponding to SPQ fluorescence changes of Calu-3 cells incubated with CSE or DMSO. The slopes were calculated from the linear regressions of the first 6 points after CFTR stimulation and were plotted as percentage (%) relative to controls. All data were expressed as mean  $\pm$  SEM. \*\* indicates  $p < 0.01$  and \*  $p < 0.05$ , as compared to control cells. Statistical analyses were performed by ANOVA and Tukey's test.

### 3.3. Effect of CSE on proinflammatory cytokines IL-6 and IL-8

To test if the cigarette smoke extract (CSE) induces a proinflammatory response in Calu-3 cells, the IL-6 and IL-8 secretion were

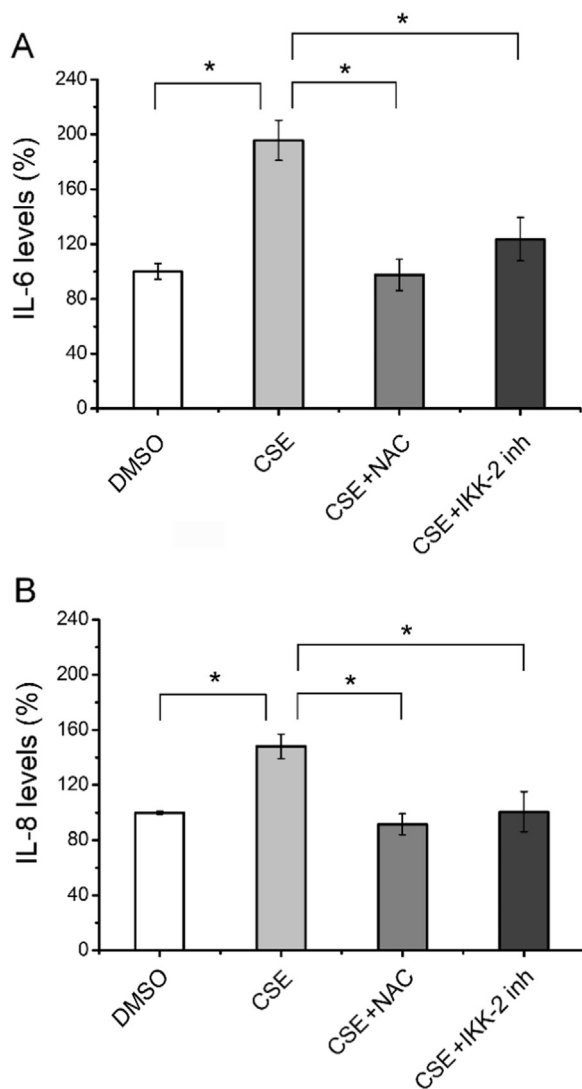


**Fig. 3. CSE induces IL-8 and IL-6 secretion through NF-κB activation.** The effect of CSE on the proinflammatory cytokines IL-8 and IL-6 secretion was evaluated by ELISA in Calu-3 cells incubated with 100 μg/ml CSE (CSE) for 24 h. The role of the increased ROS production in the IL-6/IL-8 secretion was tested by incubating with 100 μg/ml CSE + 5 mM NAC (CSE+NAC). Calu-3 cells were incubated in presence of 100 μg/ml CSE and 10 μM IKK-2 inhibitor (CSE+IKK-2 inh) to block the NF-κB signal. A) IL-8 and IL-6 (B) secretion were plotted as percentage compared to control cells as 100% and expressed as mean ± SEM. \* p < 0.05. Statistical analyses were performed by ANOVA and Tukey's test.

measured on the cultured media after 24 h incubation. We also tested if the treatment with the commonly used antioxidant NAC could protect Calu-3 cells against the CSE oxidative response as occurs in other model systems [19,23].

As shown in Figs. 3A and 3B, a significant (p < 0.01) increase in the IL-6 (3A) and IL-8 (3B) secretion was observed in cells treated with CSE (100 μg/ml, 24 h) compared to control cells (vehicle treated cells). Noteworthy, the NAC treatment completely reverted the CSE effects, showing the treated cells similar levels of IL-6 and IL-8 to those observed in control cells. These data suggest that cytokine induction by CSE was caused by increased cellular ROS levels.

It is known that the expression of proinflammatory cytokines is regulated by the transcription factor NF-κB [35–37], and that its activation can be induced by increased ROS levels [38–42]. To test if the increased IL-6 and IL-8 secretion caused by CSE through ROS was mediated by the NF-κB, Calu-3 cells were incubated with CSE in presence of 10 μM of the NF-κB pathway inhibitor IKK-2. Co-treatment of

CSE and IKK2 decreased IL-6 and IL-8 secretion compared to Calu-3 cells treated with CSE alone (Figs. 3A and 3B), suggesting that NF-κB is also involved in the activation by CSE of both cytokines, IL-6 and IL-8.

### 3.4. CSE increased cellular ROS

Cellular ROS (cROS) levels were measured in cells exposed to CSE by using the fluorescent probe DCFH-DA. As shown in Fig. 4A, the fluorescence observed by confocal microscopy in cells exposed to CSE increased and was highly diffused throughout the cells. On the other hand, NAC (5 mM) completely blocked the CSE-induced cROS. Some remaining fluorescence was observed in NAC treated cells, indicated by arrows in Fig. 4A. To quantify these responses, the DCF fluorescence was measured by using a microplate reader. In agreement with the confocal images, the ROS levels were significantly increased in cells treated with CSE for 1 h compared to control cells (p < 0.05) (Fig. 4B). In addition, the presence of NAC 5 mM reduces the CSE-induced cROS (Fig. 4B). These results are in agreement with the response of IL-6 and IL-8 to CSE and NAC (Fig. 3).

### 3.5. CSE increased mitochondrial ROS

To study the effects of CSE over mitochondrial ROS levels, we used the mtROS probe MitoSOX and performed a live time-series analysis in the presence of vehicle, CSE (100 μg/ml) or CSE (100 μg/ml) CSE plus NAC (5 mM). As shown in Fig. 5A (photograph) and 5B (quantification of images fluorescence), it was observed a fast increase (within 5 min) in the mtROS production in cells exposed to CSE. The MitoSOX fluorescence intensity in cells treated with CSE plus NAC showed a partial attenuation by NAC after 5 min, which was not longer significant after 10 min (Fig. 5B). This reduction could be due in part to the presence of some MitoSOX in cytoplasm (since a high concentration of 5 μM MitoSOX was used) [43]. However, most of the signal is not reduced by NAC and this is more evident after 10 min. The lack of NAC effectiveness to reduce the CSE-induced mtROS suggests that NAC cannot reach mitochondria at levels enough to reduce mtROS.

High mtROS levels impair the correct functioning of the mitochondrial proteins and cause mtDNA damage by oxidation [15,44,45]. Thus, the impairment of the oxidative phosphorylation system (OXPHOS) by oxidation of some major components, such as the mitochondrial Complex I and III, might cause a vicious circle of ROS production that could extend the oxidative damage [15,46]. To test if CSE exposure caused an impairment in the OXPHOS, the NADH-cytochrome c reductase (mCx-I-III) activity was measured. Mitochondria were isolated from Calu-3 cells incubated in the presence of vehicle, 100 μg/ml CSE or 100 μg/ml CSE plus 5 mM NAC for 24 h. As shown in Fig. 5C, the mCx-I-III activity decreased (p < 0.05, n = 3) in cells exposed to CSE as compared to control cells. Interestingly, NAC treatment was not able to block the effect of CSE on the mCx-I-III activity (Fig. 5C).

## 4. Discussion

The aim of this work was study the effects of NAC treatment over the proinflammatory response produced by CSE in the epithelial airway cells Calu-3, used as a simplified *in vitro* model for COPD [25]. The results obtained are summarized in Fig. 6, together with the possible mechanisms involved. Using a CSE concentration and incubation time of 100 μg/ml during 24 h, no significant effects over cells survival were observed, and this concentration and time were used in subsequent experiments. CFTR mRNA expression and activity were significantly reduced after CSE exposure, in agreement with previous results from other laboratories in diverse model systems, showing deleterious effects of CSE on CFTR activity [1,6–12,47]. Thus, these results suggest that Calu-3 cells are a good model system for COPD studies.

Using this model system, we observed increased IL-6 and IL-8 levels

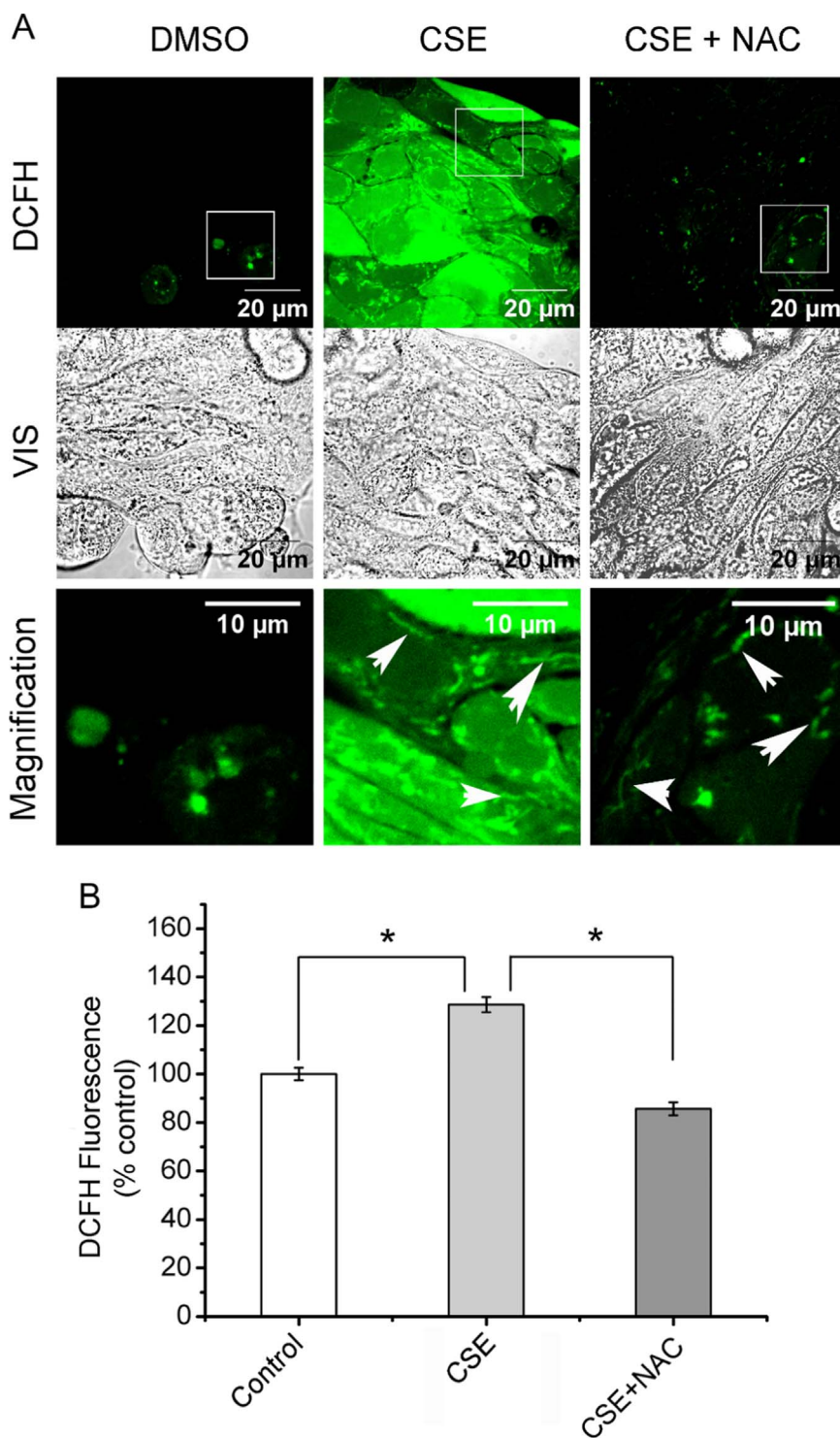


**Fig. 4. Cellular ROS increase by CSE exposure and NAC protection.** A) Confocal image of total cellular ROS levels measured by using DCFH-DA, in cells treated with CSE or CSE + NAC for 1 h. Images were acquired by using a Plan-Neofluar 100 × /1.3 Oil objective, a laser line of 488 nm, and a LP filter of 505 nm. VIS indicates the visible (transmitted light) image of cells. Magnifications corresponded to the white squares indicated in the figures. Arrows indicates regions of intracellular accumulation of ROS. B: Spectrofluorometry of cellular ROS levels measured by using DCFH-DA in cells incubated with 100 μg/ml CSE (CSE), DMSO or 100 μg/ml CSE + 5 mM NAC (CSE + NAC) for 1 h.

after CSE exposure. Interestingly, this response was totally reverted by treatment with NAC, suggesting that a ROS signaling, induced by CSE, is involved in the production of these proinflammatory cytokines. This is in agreement with prior publications in other model systems [19,48–51]. It is important to highlight that the increased cytokine levels were induced directly by CSE, in absence of bacterial infection (aseptic or sterile inflammation) or LPS stimulation, as it has been proposed by other authors [19,48]. Zhou et al. [51] identified different

CSE compounds that could induce the production of IL-8 in human epithelium bronchial 16HBE cells, suggesting that the chemical composition of the CSE could start the inflammatory phenotype in COPD, previously to any bacterial infection. Also, Ko et al. observed that CSE exposure induces IL-8 release from macrophages mediated by ROS activation of NF-κB through the AMP-activated protein kinase (AMPK). NAC treatment also attenuated the IL-8 induction [49].

Measuring the DCF fluorescence, a significant increase in ROS

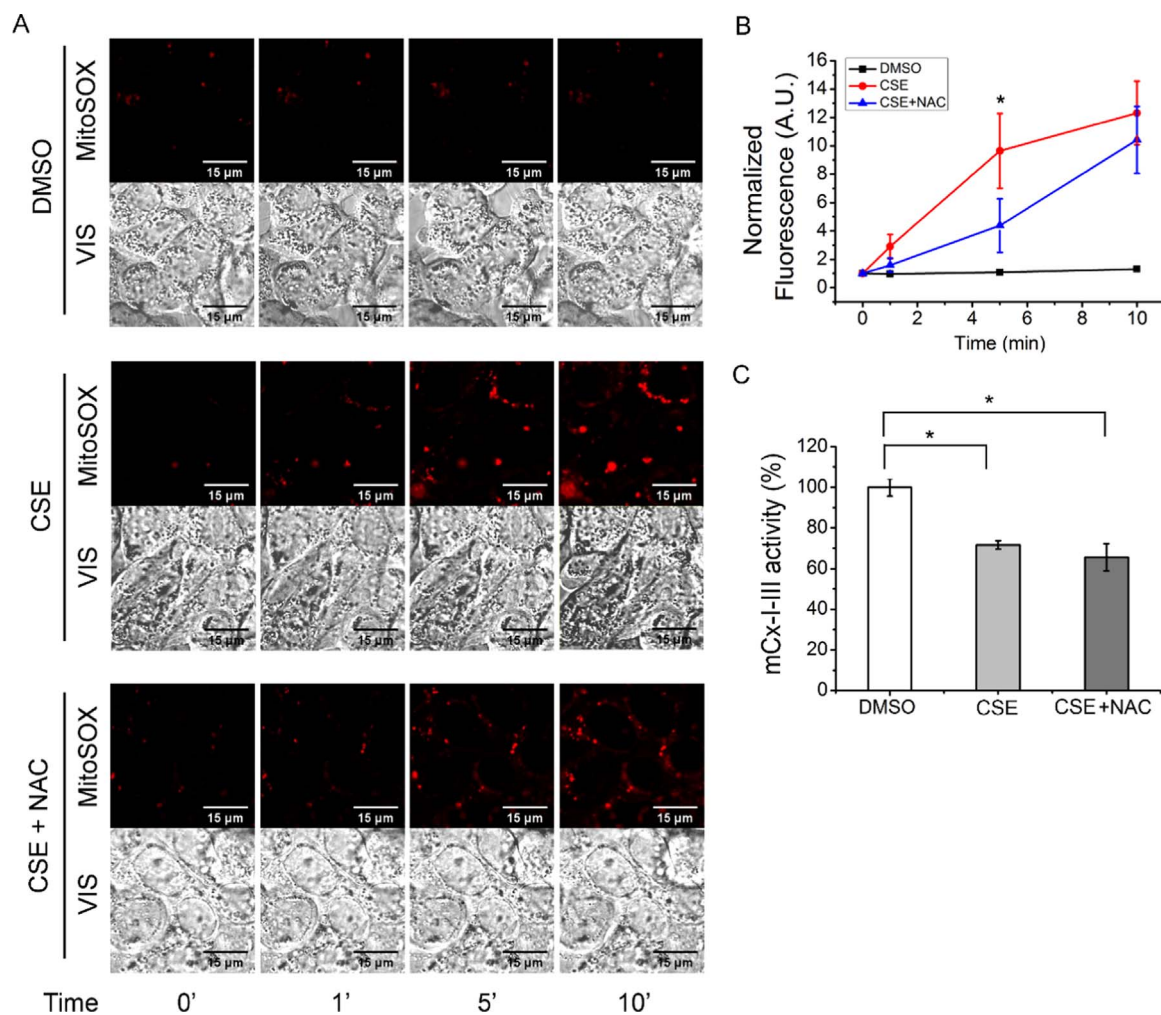


**Fig. 5. Effects of CSE on mitochondrial ROS levels and Complex I-III activity.** A) Confocal microscopy corresponding to mitochondrial ROS (mtROS) levels measured by using MitoSOX at different times (0, 1, 5 and 10 min) in the presence of 100 µg/ml of CSE. Images were taken by using the time series configuration of the LSM 510 confocal microscope, a Plan-Neofluar 100 ×/1.3 Oil objective, a laser filter of 488 nm, and a LP filter of 560 nm. VIS indicates the visible image of cells. B) Normalized MitoSOX fluorescence values of corrected total cell fluorescence (CTCF) corresponding to the images shown in A. Fluorescence was normalized relative to control cells. C: Mitochondrial NADH-cytochrome c reductase (mCx-I-III) measured in Calu-3 cells incubated with 100 µg/ml CSE (CSE), DMSO or 100 µg/ml CSE + 5 mM NAC (CSE + NAC) for 24 h. Data were expressed as mean ± SEM of three independent experiments (n = 3). \* indicates p < 0.05 compared to CSE-treated cells. Statistical analyses were performed by ANOVA and Tukey's test.

production was observed in Calu-3 cells treated with CSE (100 µg/ml) for 1 h. Interestingly, NAC (5 mM) was able to completely block this effect, as occurred with the IL-6 and IL-8 secretion. On the other hand, the mitochondrial ROS (mtROS) production, measured by using MitoSOX, also increased very rapidly after the CSE treatment (in less than 5 min). The NAC treatment produced a partial attenuation in the MitoSOX signal, significant at 5 min, which could be in part due to some MitoSOX accumulated in the cytoplasm [43]. However, the NAC treatment was insufficient to completely block the induced mtROS at 5 min and after 10 min the differences were no longer significant.

In addition to the increased mtROS production, after 24 h of exposure to 100 µg/ml CSE, it was observed a decreased mCx-I-III activity that was not reverted by NAC exposure. These data suggest that this antioxidant treatment was not effective to block and protect key components of the mitochondrial OXPHOS (or that NAC by itself affects the mCx-I-III activity). Several reports suggest that the inhibition of mCx-I cause increased ROS levels in some diseases [52,53]. In fact, it has been previously observed a reduced mCx-I activity and increased ROS production in cells with impaired CFTR activity [13–15,27,54]. The fast mtROS induction observed with CSE (< 5 min) suggests that the reduction in the CFTR activity and expression, as well as the reduction in the mCx-I-III activity, occur after the increase in ROS levels. However, the specific role of CFTR regarding the inflammatory response induced

by CSE is not clear yet, since NAC could not revert the low CFTR levels induced by CSE, although it normalized the IL-6 and IL-8 levels. Thus, the reduced CFTR levels could be just a consequence of the CSE treatment, and not the cause for the increased IL-6 and IL-8 levels. Since the CFTR failure increases IL-1β levels and decreases mCx-I-III activity [13,55], CFTR might have some role in the CSE-induced proinflammatory state and mitochondrial failure, that is not corrected by NAC treatment. In fact, NAC treatment also failed to normalize the CFTR levels. A CFTR correction, normalizing the mCx-I-III and ROS activities, might therefore be of clinical relevance for COPD treatment [56,57], perhaps accompanied by NAC treatment. However, further research is needed to better understand the complex mechanisms involved in the CFTR down-regulation and signaling [27,55,58–65], and particularly under CSE exposure.

We conclude that Calu-3 cells constitute an appropriate *in vitro* model to study the effects of CSE on oxidative and proinflammatory responses. A very rapid oxidative stress is developed under CSE exposure, which initiates a sterile proinflammatory response, affecting also the mitochondrial function, the CFTR levels, and causing changes in ROS production (illustrated in Fig. 6). NAC treatment could inhibit the CSE cytoplasmic effects on ROS and cytokines, although the mitochondrial effects on ROS were only partially reverted and NAC had no effects on the reduced mCx-I-III activity. Other inhibitors able to

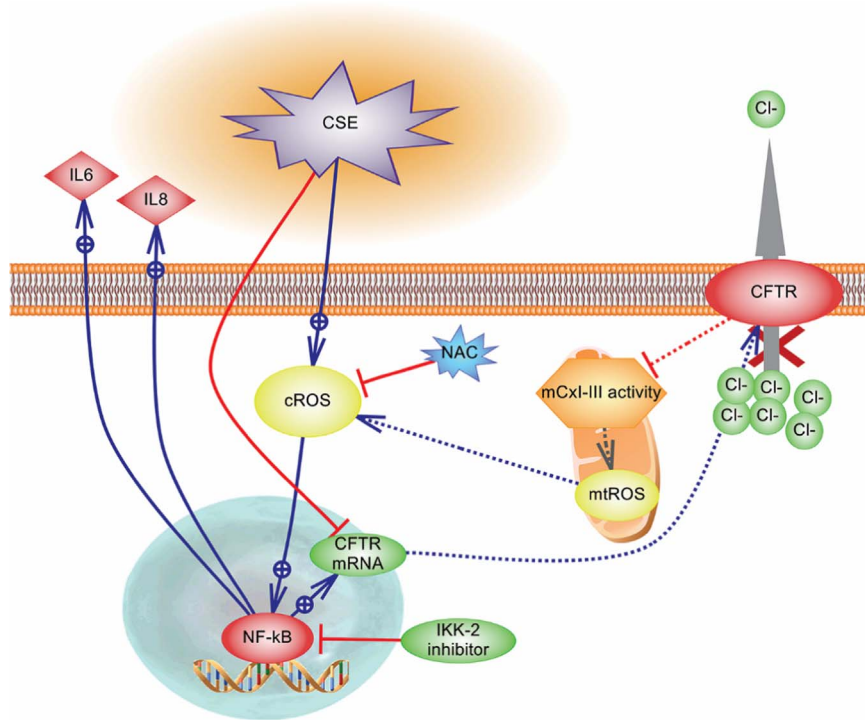


**Fig. 6.** CSE effects on Calu-3 cells. The figure illustrates the effects of CSE in CFTR expression and activity, the mCx-I-III inhibition, the increased cROS and mtROS production, the pro-inflammatory response as IL-6 and IL-8 secretion, and the possible mechanisms involved. The cytoplasmic effects of CSE were reverted by incubations with NAC or NF-κB inhibitor (IKK-2 inhibitor). The NAC treatment inhibited cROS production whereas was not enough to effectively block mtROS production (green solid line -) or to revert the mCx-I-III activity. Stimulations: blue line and arrow; inhibitions; red line and -|. The illustration shows the results obtained here (solid lines) and the postulated mechanisms (dotted lines). (For interpretation of the references to color in this figure legend, the reader is referred to the web version of this article.)

circumvent the mitochondrial failure and the low CFTR levels could be useful to avoid exacerbations in COPD.

**Acknowledgments**

We thank Professor Diego Battiato and Romina D’Agostino for administrative assistance, and the technical assistant of María de los Angeles Aguilar.

**Funding**

This work was supported by the National Agency for the Promotion of Science and Technology (ANPCYT) [grant number PICT 2012-1278] to TASC, and [grant number PICT-2015-1031] to AGV; the National Scientific and Technical Research Council (CONICET) [PIP 2015 11220150100227, and P-UE 2016 22920160100129CO] to TASC; a grant from the Pontifical Catholic University of Argentina (UCA) to TASC, and research fellowships from CONICET to MC. This work was also supported by Fundación Pablo Cassará.

**Appendix A. Supporting information**

Supplementary data associated with this article can be found in the online version at <http://dx.doi.org/10.1016/j.redox.2018.03.006>.

**References**

[1] A. Rab, S.M. Rowe, S.V. Raju, Z. Bebok, S. Matalon, J.F. Collawn, Cigarette smoke and CFTR: implications in the pathogenesis of COPD, *Am. J. Physiol. Lung Cell. Mol. Physiol.* 305 (2013) L530–L541.  
 [2] A.J. Mehta, D. Miedinger, D. Keidel, R. Bettschart, A. Bircher, P.O. Bridevaux, I. Curjuric, H. Kromhout, T. Rochat, T. Rothe, et al., Occupational exposure to dusts, gases, and fumes and incidence of chronic obstructive pulmonary disease in the Swiss Cohort Study on Air Pollution and Lung and Heart Diseases in Adults, *Am. J. Respir. Crit. Care Med.* 185 (2012) 1292–1300.  
 [3] P. Fanen, A. Wohlhuter-Haddad, A. Hinzpeter, Genetics of cystic fibrosis: cfr mutation classifications toward genotype-based CF therapies, *Int. J. Biochem. Cell Biol.* 52 (2014) 94–102.  
 [4] J.R. Riordan, J.M. Rommens, B. Kerem, N. Alon, R. Rozmahel, Z. Grzelczak, J. Zielenski, S. Lok, N. Plavsic, J.L. Chou, et al., Identification of the cystic fibrosis gene: cloning and characterization of complementary DNA, *Science* 245 (1989)

1066–1073.  
 [5] J.M. Rommens, M.C. Iannuzzi, B. Kerem, M.L. Drumm, G. Melmer, M. Dean, R. Rozmahel, J.L. Cole, D. Kennedy, N. Hidaka, et al., Identification of the cystic fibrosis gene: chromosome walking and jumping, *Science* 245 (1989) 1059–1065.  
 [6] S.V. Raju, P.L. Jackson, C.A. Courville, C.M. McNicholas, P.A. Sloane, G. Sabbatini, S. Tidwell, L.P. Tang, B. Liu, J.A. Fortenberry, et al., Cigarette smoke induces systemic defects in cystic fibrosis transmembrane conductance regulator function, *Am. J. Respir. Crit. Care Med.* 188 (2013) 1321–1330.  
 [7] X. Xu, R. Balsiger, J. Tyrrell, P.N. Boyaka, R. Tarran, E. Cormet-Boyaka, Cigarette smoke exposure reveals a novel role for the MEK/ERK1/2 MAPK pathway in regulation of CFTR, *Biochim. Biophys. Acta* 1850 (2015) 1224–1232.  
 [8] A.R. Moran, Y. Norimatsu, D.C. Dawson, K.D. MacDonald, Aqueous cigarette smoke extract induces a voltage-dependent inhibition of CFTR expressed in *Xenopus* oocytes, *Am. J. Physiol. Lung Cell. Mol. Physiol.* 306 (2014) L284–L291.  
 [9] J.E. Rasmussen, J.T. Sheridan, W. Polk, C.M. Davies, R. Tarran, Cigarette smoke-induced Ca<sup>2+</sup> release leads to cystic fibrosis transmembrane conductance regulator (CFTR) dysfunction, *J. Biol. Chem.* 289 (2014) 7671–7681.  
 [10] F. Hassan, X. Xu, G. Nuovo, D.W. Killilea, J. Tyrrell, C. Da Tan, R. Tarran, P. Diaz, J. Jee, D. Knoell, et al., Accumulation of metals in GOLD4 COPD lungs is associated with decreased CFTR levels, *Respir. Res.* 15 (2014) 69.  
 [11] L.A. Clunes, C.M. Davies, R.D. Coakley, A.A. Aleksandrov, A.G. Henderson, K.L. Zeman, E.N. Worthington, M. Gentsch, S.M. Kreda, D. Cholon, et al., Cigarette smoke exposure induces CFTR internalization and insolubility, leading to airway surface liquid dehydration, *FASEB J.* 26 (2012) 533–545.  
 [12] A.M. Cantin, J.W. Hanrahan, G. Bilodeau, L. Ellis, A. Dupuis, J. Liao, J. Zielenski, P. Durie, Cystic fibrosis transmembrane conductance regulator function is suppressed in cigarette smokers, *Am. J. Respir. Crit. Care Med.* 173 (2006) 1139–1144.  
 [13] M. Clazure, A.G. Valdivieso, M.M. Massip Copiz, G. Schulman, M.L. Teiber, T.A. Santa-Coloma, Disruption of interleukin-1beta autocrine signaling rescues complex I activity and improves ROS levels in immortalized epithelial cells with impaired cystic fibrosis transmembrane conductance regulator (CFTR) function, *PLoS One* 9 (2014) e99257.  
 [14] M. Kelly-Aubert, S. Trudel, J. Fritsch, T. Nguyen-Khoa, M. Baudouin-Legros, S. Moriceau, L. Jeanson, F. Djouadi, C. Matar, M. Conti, et al., GSH monoethyl ester rescues mitochondrial defects in cystic fibrosis models, *Hum. Mol. Genet.* (2011).  
 [15] A.G. Valdivieso, T.A. Santa-Coloma, CFTR activity and mitochondrial function, *Redox Biol.* 1 (2013) 190–202.  
 [16] L.W. Velsor, C. Kariya, R. Kachadourian, B.J. Day, Mitochondrial oxidative stress in the lungs of cystic fibrosis transmembrane conductance regulator protein mutant mice, *Am. J. Respir. Cell Mol. Biol.* 35 (2006) 579–586.  
 [17] A.G. Valdivieso, M. Clazure, M.C. Marin, G.L. Taminelli, M.M. Massip Copiz, F. Sanchez, G. Schulman, M.L. Teiber, T.A. Santa-Coloma, The mitochondrial complex I activity is reduced in cells with impaired cystic fibrosis transmembrane conductance regulator (CFTR) function, *PLoS One* 7 (2012) e48059.  
 [18] C. Duranton, I. Rubera, M. Coughnon, N. Melis, A. Chargui, B. Mograbi, M. Tauc, CFTR is involved in the fine tuning of intracellular redox status: physiological implications in cystic fibrosis, *Am. J. Pathol.* 181 (2012) 1367–1377.  
 [19] M. Cazzola, L. Calzetta, F. Facciolo, P. Rogliani, M.G. Matera, Pharmacological investigation on the anti-oxidant and anti-inflammatory activity of N-acetylcysteine in an ex vivo model of COPD exacerbation, *Respir. Res.* 18 (2017) 26.



[20] A.M. Sadowska, J. Verbraecken, K. Darquennes, W.A. De Backer, Role of N-acetylcysteine in the management of COPD, *Int. J. Chronic Obstr. Pulm. Dis.* 1 (2006) 425–434.

[21] M.G. Matera, L. Calzetta, M. Cazzola, Oxidation pathway and exacerbations in COPD: the role of NAC, *Expert Rev. Respir. Med.* 10 (2016) 89–97.

[22] K.R. Atkuri, J.J. Mantovani, L.A. Herzenberg, L.A. Herzenberg, N-Acetylcysteine—a safe antidote for cysteine/glutathione deficiency, *Curr. Opin. Pharmacol.* 7 (2007) 355–359.

[23] C.M. Sanguinetti, N-acetylcysteine in COPD: why, how, and when? *Multidiscip. Respir. Med.* 11 (2015) 8.

[24] B. Shen, W. Finkbeiner, J. Wine, R. Mrsny, J. Widdicombe, Calu-3: a human airway epithelial cell line that shows cAMP-dependent Cl-secretion, *Am. J. Physiol.-Lung Cell. Mol. Physiol.* 266 (1994) L493–L501.

[25] Y. Zhu, A. Chidekel, T.H. Shaffer, Cultured human airway epithelial cells (calu-3): a model of human respiratory function, structure, and inflammatory responses, *Crit. Care Res. Pract.* 2010 (2010).

[26] G. Da Violante, N. Zerrouk, I. Richard, G. Provot, J.C. Chaumeil, P. Arnaud, Evaluation of the cytotoxicity effect of dimethyl sulfoxide (DMSO) on Caco2/TC7 colon tumor cell cultures, *Biol. Pharm. Bull.* 25 (2002) 1600–1603.

[27] M.M. Massip-Copiz, M. Clauzure, A.G. Valdivieso, T.A. Santa-Coloma, CFTR impairment upregulates c-Src activity through IL-1beta autocrine signaling, *Arch. Biochem. Biophys.* 616 (2017) 1–12.

[28] A.G. Valdivieso, M.C. Marin, M. Clauzure, T.A. Santa-Coloma, Measurement of cystic fibrosis transmembrane conductance regulator activity using fluorescence spectrophotometry, *Anal. Biochem.* 418 (2011) 231–237.

[29] R.A. McCloy, S. Rogers, C.E. Caldon, T. Lorca, A. Castro, A. Burgess, Partial inhibition of Cdk1 in G2 phase overrides the SAC and decouples mitotic events, *Cell Cycle* 13 (2014) 1400–1412.

[30] A. Burgess, S. Vigneron, E. Brioudes, J.C. Labbe, T. Lorca, A. Castro, Loss of human Greatwall results in G2 arrest and multiple mitotic defects due to deregulation of the cyclin B-Cdc2/PP2A balance, *Proc. Natl. Acad. Sci. USA* 107 (2010) 12564–12569.

[31] A. Majander, K. Huoponen, M.L. Savontaus, E. Nikoskelainen, M. Wikstrom, Electron transfer properties of NADH:ubiquinone reductase in the ND1/3460 and the ND4/11778 mutations of the Leber hereditary optic neuroretinopathy (LHON), *FEBS Lett.* 292 (1991) 289–292.

[32] O.H. Lowry, N.J. Rosebroug, A.L. Farr, R.J. Randall, Protein measurement with the Folin phenol reagent, *J. Biol. Chem.* 193 (1951) 265–275.

[33] A.K. Joshi, N. Raju, P.S. Rajini, Microplate-based kinetic method for assay of mitochondrial NADH- and succinate-cytochrome c reductase activities, *Anal. Biochem.* 415 (2011) 209–211.

[34] A. Navarro, M.J. Bandez, C. Gomez, M.G. Repetto, A. Boveris, Effects of rotenone and pyridaben on complex I electron transfer and on mitochondrial nitric oxide synthase functional activity, *J. Bioenergy Biomembr.* 42 (2010) 405–412.

[35] P.P. Tak, G.S. Firestein, NF-kappaB: a key role in inflammatory diseases, *J. Clin. Invest.* 107 (2001) 7–11.

[36] T. Lawrence, The nuclear factor NF-kappaB pathway in inflammation, *Cold Spring Harb. Perspect. Biol.* 1 (2009) a001651.

[37] C. Schmidt, B. Peng, Z. Li, G.M. Scwab, S. Fujioka, J. Niu, M. Schmidt-Supprian, D.B. Evans, J.L. Abbruzzese, P.J. Chiao, Mechanisms of proinflammatory cytokine-induced biphasic NF-kappaB activation, *Mol. Cell* 12 (2003) 1287–1300.

[38] P. Brennan, L.A. O'Neill, Effects of oxidants and antioxidants on nuclear factor kappa B activation in three different cell lines: evidence against a universal hypothesis involving oxygen radicals, *Biochim. Biophys. Acta* 1260 (1995) 167–175.

[39] M.J. Morgan, Z.G. Liu, Crosstalk of reactive oxygen species and NF-kappaB signaling, *Cell Res.* 21 (2011) 103–115.

[40] M. Imran, I.K. Lim, Regulation of Btg2(TIS21/PC3) expression via reactive oxygen species-protein kinase C-NuKappaBeta pathway under stress conditions, *Cell. Signal.* 25 (2013) 2400–2412.

[41] M. Hayakawa, H. Miyashita, I. Sakamoto, M. Kitagawa, H. Tanaka, H. Yasuda, M. Karin, K. Kikugawa, Evidence that reactive oxygen species do not mediate NF-kappaB activation, *EMBO J.* 22 (2003) 3356–3366.

[42] T. Liu, L. Wu, D. Wang, H. Wang, J. Chen, C. Yang, J. Bao, C. Wu, Role of reactive oxygen species-mediated MAPK and NF-kappaB activation in polyonatum cyrtoma lectin-induced apoptosis and autophagy in human lung adenocarcinoma A549 cells, *J. Biochem.* 160 (2016) 315–324.

[43] S.I. Dikalov, D.G. Harrison, Methods for detection of mitochondrial and cellular reactive oxygen species, *Antioxid. Redox Signal.* 20 (2014) 372–382.

[44] F.Q. Liang, B.F. Godley, Oxidative stress-induced mitochondrial DNA damage in human retinal pigment epithelial cells: a possible mechanism for RPE aging and age-related macular degeneration, *Exp. Eye Res.* 76 (2003) 397–403.

[45] P.A. Kramer, V.M. Darley-Usmar, The emerging theme of redox bioenergetics in health and disease, *Biomed. J.* 38 (2015) 294–300.

[46] M.L. Genova, G. Lenaz, The interplay between respiratory supercomplexes and ROS in aging, *Antioxid. Redox Signal.* 23 (2015) 208–238.

[47] Z. Bebok, K. Varga, J.K. Hicks, C.J. Venglarik, T. Kovacs, L. Chen, K.M. Hardiman, J.F. Collawn, E.J. Sorscher, S. Matalon, Reactive oxygen nitrogen species decrease cystic fibrosis transmembrane conductance regulator expression and cAMP-mediated Cl- secretion in airway epithelia, *J. Biol. Chem.* 277 (2002) 43041–43049.

[48] D.M. Comer, J.S. Elborn, M. Ennis, Inflammatory and cytotoxic effects of acrolein, nicotine, acetaldehyde and cigarette smoke extract on human nasal epithelial cells, *BMC Pulm. Med.* 14 (2014) 32.

[49] H.K. Ko, H.F. Lee, A.H. Lin, M.H. Liu, C.I. Liu, T.S. Lee, Y.R. Kou, Regulation of cigarette smoke induction of IL-8 in macrophages by AMP-activated protein kinase signaling, *J. Cell. Physiol.* 230 (2015) 1781–1793.

[50] Y.P. Wu, C. Cao, Y.F. Wu, M. Li, T.W. Lai, C. Zhu, Y. Wang, S.M. Ying, Z.H. Chen, H.H. Shen, et al., Activating transcription factor 3 represses cigarette smoke-induced IL6 and IL8 expression via suppressing NF-kappaB activation, *Toxicol. Lett.* 270 (2017) 17–24.

[51] G. Zhou, W. Xiao, C. Xu, Y. Hu, X. Wu, F. Huang, X. Lu, C. Shi, X. Wu, Chemical constituents of tobacco smoke induce the production of interleukin-8 in human bronchial epithelium, 16HBE cells, *Tob. Induc. Dis.* 14 (2016) 24.

[52] S. Pitkanen, B.H. Robinson, Mitochondrial complex I deficiency leads to increased production of superoxide radicals and induction of superoxide dismutase, *J. Clin. Invest.* 98 (1996) 345–351.

[53] B.H. Robinson, Human Complex I deficiency: clinical spectrum and involvement of oxygen free radicals in the pathogenicity of the defect, *Biochim. Biophys. Acta* 1364 (1998) 271–286.

[54] A. Atlante, M. Favia, A. Bobba, L. Guerra, V. Casavola, S.J. Reshkin, Characterization of tobacco smoke induce the production of interleukin-8 in human bronchial epithelium, 16HBE cells, *Tob. Induc. Dis.* 14 (2016) 24.

[55] M. Clauzure, A.G. Valdivieso, M.M. Massip-Copiz, C. Mori, A.V. Dugour, J.M. Figueroa, T.A. Santa-Coloma, Intracellular chloride concentration changes modulate IL-1beta expression and secretion in human bronchial epithelial cultured cells, *J. Cell. Biochem.* (2016).

[56] S.V. Raju, V.Y. Lin, L. Liu, C.M. McNicholas, S. Karki, P.A. Sloane, L. Tang, P.L. Jackson, W. Wang, L. Wilson, et al., The cystic fibrosis transmembrane conductance regulator potentiator ivacaftor augments mucociliary clearance abrogating cystic fibrosis transmembrane conductance regulator inhibition by cigarette smoke, *Am. J. Respir. Cell Mol. Biol.* 56 (2017) 99–108.

[57] G.M. Solomon, S.V. Raju, M.T. Dransfield, S.M. Rowe, Therapeutic approaches to acquired cystic fibrosis transmembrane conductance regulator dysfunction in chronic bronchitis, *Ann. Am. Thorac. Soc.* 13 (Suppl. 2) (2016) S169–S176.

[58] E.G. Cafferata, A.M. Guericco, O.H. Pivetta, T.A. Santa-Coloma, NF-kappaB activation is involved in regulation of cystic fibrosis transmembrane conductance regulator (CFTR) by interleukin-1beta, *J. Biol. Chem.* 276 (2001) 15441–15444.

[59] E.G. Cafferata, A.M. Gonzalez-Guerrico, L. Giordano, O.H. Pivetta, T.A. Santa-Coloma, Interleukin-1beta regulates CFTR expression in human intestinal T84 cells, *Biochim. Biophys. Acta* 1500 (2000) 241–248.

[60] A.M. Gonzalez-Guerrico, E.G. Cafferata, M. Radrizzani, F. Marcucci, D. Gruenert, O.H. Pivetta, R.R. Favaloro, R. Laguens, S.V. Perrone, G.C. Gallo, et al., Tyrosine kinase c-Src constitutes a bridge between cystic fibrosis transmembrane regulator channel failure and MUC1 overexpression in cystic fibrosis, *J. Biol. Chem.* 277 (2002) 17239–17247.

[61] M. Massip-Copiz, M. Clauzure, A.G. Valdivieso, T.A. Santa-Coloma, Epieregulin (EREG) is upregulated through an IL-1beta autocrine loop in Caco-2 epithelial cells with reduced CFTR function, *J. Cell. Biochem.* 119 (2018) 2911–2922.

[62] A.G. Valdivieso, C. Mori, M. Clauzure, M. Massip-Copiz, T.A. Santa-Coloma, CFTR modulates RPS27 gene expression using chloride anion as signaling effector, *Arch. Biochem. Biophys.* 633 (2017) 103–109.

[63] M.M. Massip Copiz, T.A. Santa Coloma, C- Src and its role in cystic fibrosis, *Eur. J. Cell Biol.* 95 (2016) 401–413.

[64] M. Clauzure, A.G. Valdivieso, M.M. Massip-Copiz, C. Mori, A.V. Dugour, J.M. Figueroa, T.A. Santa-Coloma, Intracellular chloride concentration changes modulate IL-1beta expression and secretion in human bronchial epithelial cultured cells, *J. Cell. Biochem.* 118 (2017) 2131–2140.

[65] A.G. Valdivieso, M. Clauzure, M. Massip-Copiz, T.A. Santa-Coloma, The chloride anion acts as a second messenger in mammalian cells - modifying the expression of specific genes, *Cell. Physiol. Biochem.: Int. J. Exp. Cell. Physiol., Biochem., Pharmacol.* 38 (2016) 49–64.